15ÈMES JOURNÉES DE L'HYDRODYNAMIQUE
22 - 24 novembre 2016 - Brest

ETUDE EXPERIMENTALE A TRES PETITE ECHELLE DU COMPORTEMENT DYNAMIQUE D'UN FLOTTEUR D'EOLIENNE FLOTTANTE

ON THE INTEREST OF VERY SMALL-SCALE WAVE BASIN TESTS FOR THE DESCRIPTION OF FLOATING WIND TURBINE DYNAMICS

C. GROUTHIER[(1)*], R. ANTONUTTI[(2)(3)], C. PEYRARD[(2)(3)], O. DOARE[(4)], C. BARRAUD[(1)(4)(5)]

(1) Wood Group, 15-19 rue des Mathurins, 75009 PARIS, FRANCE
(2) EDF R&D – Electricité de France Research and Development, 6 quai Watier, 78400 CHATOU, FRANCE
(3) Saint-Venant Hydraulics Laboratory, Université Paris-Est, 6 quai Watier, 78400 CHATOU, FRANCE
(4) IMSIA, ENSTA ParisTech, CNRS, CEA, EDF, Université Paris-Saclay, 828 boulevard des Maréchaux, 91762 PALAISEAU CEDEX, FRANCE
(5) Laboratorio de Estudios Avanzados en Fenómenos No Lineales, Facultad de Ciencias Físicas y Matemáticas, Universidad de Chile, Beauchef 850, SANTIAGO, CHILE
* *Corresponding author : Clement.Grouthier@woodgroup.com*

Résumé

Les installations permettant de mener des campagnes d'essais sur des éoliennes flottantes à des échelles de l'ordre de 1/20ème à 1/100ème sont rares. Il parait dès lors intéressant de se poser la question de l'intérêt d'essais à très petite échelle, inférieure au 1/100ème, pour gagner en compréhension de la dynamique des flotteurs sans avoir à mobiliser de très lourds moyens d'essais. L'étude présentée dans cet article vise à évaluer les informations que l'on peut tirer de telles expériences, grâce à une comparaison entre une analyse expérimentale à très petite échelle, 1/500ème, et une analyse numérique à l'échelle 1. L'accord entre les deux méthodes au niveau de la dynamique du flotteur semble donner du crédit à ces essais à très petite échelle. Néanmoins, un si petit facteur d'échelle introduit des différences fondamentales entre les essais et la réalité, qui sont discutées en fin d'article et qu'il convient de prendre en compte lors de futures essais en bassin à très petite échelle.

Abstract

Facilities allowing for experimental campaigns on floating wind turbines at scales between 1/20th and 1/100th are rare. It is consequently interesting to investigate the interest of wave basin tests at very small-scale, i.e. less than 1/100th, to gain in the understanding of such floating structures dynamics. The present study therefore aims at evaluating the information that could be gained from very small scale experiments, thanks to a comparison between wave basin tests conducted at 1/500th scale and numerical simulations at real scale. The good agreement between the measured dynamics would tend to confirm the interest of such very-small scale tests. Such a small scale yet results in some fundamental differences with the real-scale configuration, which are also discussed in this article and must be kept in mind for future very-small scale tests.

1. Introduction

The development of the offshore wind industry is part of the global effort to meet the objectives fixed by governments in terms of greenhouse gas cuts. Wind is steadier and stronger away from shore, where bigger wind turbines can be installed. The installation cost of fixed offshore wind turbines when the water depth exceeds 50 to 60 meters would however be prohibitive and floating wind turbines are therefore considered.

Many floating wind projects are currently under development, involving numerous innovative floater concepts, for which extensive design analyses are required. Innovative concepts are consequently investigated and lots of technical challenges still remain when it comes to the design of such a structure, for which both aerodynamic and hydrodynamic effects may result in significant loads. Dedicated software or numerical approaches exist, or are being developed to help in the design of these floating structures. However, no mature standards exist and the track record of the numerical tools may appear as not sufficient to circumvent the need for an experimental campaign in the validation process of a floating wind turbine design.

Wave basin tests with reduced-scale models (with scaling factors typically in the range between 1/20th and 1/100th) are actually still necessary to confirm the relevance of the selected designs and to support their certification. Not a lot of wave basins are yet big enough to deal with such models and the induced logistical effort, if not the costs or the availability of the testing facilities, apply very important constraints on those tests. As lots of smaller wave basins and flumes are available, one can therefore wonder how these could be used to support the design studies of floating wind turbines, [1]. Performing smaller scale experiments would also allow for an easier manufacturing of the model, which would be of great interest as the model would then be easy to modify/adapt when converging towards an optimal design. For sure, the small scale of the models will result in severe violations of some similitude laws and the small size of the models will impact the physical couplings driving the dynamic behaviour of the floater. It may however sound interesting to take benefit from smaller facilities to perform wave basin tests during the floater design analyses and reserve the use of big wave basins for the formal confirmation of a final design. This however requires an accurate knowledge of the interest and limitations of very small scale wave basin tests.
The present paper focuses on the interest of very small scale wave flume tests to support floating wind turbine design studies. The experimental campaign, introduced in Section 2, investigates the dynamic response of small scale floater models and aims at identifying the relevant information that can be extracted from such tests as well as their limitations. Numerical investigations considering a similar floater, carried out at the full scale and partially calibrated on small-scale parameters, were performed simultaneously, as described in Section 3. Results from both experimental and numerical analyses are then presented and compared in Section 4, before some conclusions are drawn on the interest of such small-scale tests for the understanding of the dynamic behaviour of this type of floating device, in Section 5.

2. Experimental Campaign

   a. Wave Basin Description

The experimental campaign was performed in the wave flume of ENSTA ParisTech, which is shown on Figure 1. It consists of a wave basin of 25 cm width, 8 m length, in which the water height can be up to 35 cm approximatively.

A flap is located at the upstream extremity of the wave basin and is used to generate surface waves. Practically, the flap is actuated using a strong servomotor, see Figure 2 (a), which

allows to generate an arbitrary displacement and is controlled in amplitude and frequency by the controller shown on Figure 2 (b). In practice, a sinusoidal angular displacement is imposed to the flap, so that monochromatic unidirectional travelling waves are generated. A low slope beach is placed at the downstream extremity of the basin to avoid wave reflexions and preserve the travelling behaviour of the tested waves.

b. Sensors

Two resistive wave gauges are used to measure the instantaneous free surface elevation. These sensors can be shifted along the entire length of the basin in order to measure the water height at any location along the basin. These sensors consist of two vertical wires partially submerged in water. The electrical resistance hence varies between the wires when the water height varies. A Wheatstone bridge is then used to measure the resistance between the two wires of the sensors. Typical calibrating curves of the sensors are shown on Figure 3, exhibiting the relations between the water level and the voltage across the Wheatstone bridge. The relationship between voltage and water level is finally assumed linear in the range of interest. As the resistance between the two rods of the sensors may depend on several external parameters like the ambient temperature, such calibrations were derived in parallel for every set of performed tests.

In order to track the displacements of the floating structure, a set of two cameras has been used, respectively placed aside and on top of the reduced-scale model. Figure 4 represents a typical set of images acquired by the cameras. Two light markers on the dark floating structure appear on each photograph. Before every tested wave, a picture of the static configuration is saved as a reference frame and a combination of image processing and geometrical calculations is then applied to extract displacement with respect to the center of gravity of the model out of the films captured.

a. Wave Basin Calibration

As a preliminary stage of the experimental campaign, the calibration of the wave basin is performed in order to characterize the waves generated in terms of frequency and wavelength. The derivation of the experimental dispersion relation of the waves generated in the basin is also interesting in the aim of assessing the consistency of the generated wave trains with classical wave theory, [7]. It is indeed expected that the relation dispersion follows

$$D(k,\omega) = \omega^2 - gk\tanh(kh) = 0 \qquad (1)$$

with ω and k the wave angular frequency and wavenumber, $g = 9.81\ m/s^2$ the acceleration of gravity and h the mean water depth, which is equal to 30 cm in the presented set of experiments. The dispersion relation describing the waves in the wave basin is shown on Figure 5, exhibiting a very good agreement between experimental values and the theoretical formula, eqn. (1).

Figure 1: Pictures of the wave basin used in the experiments

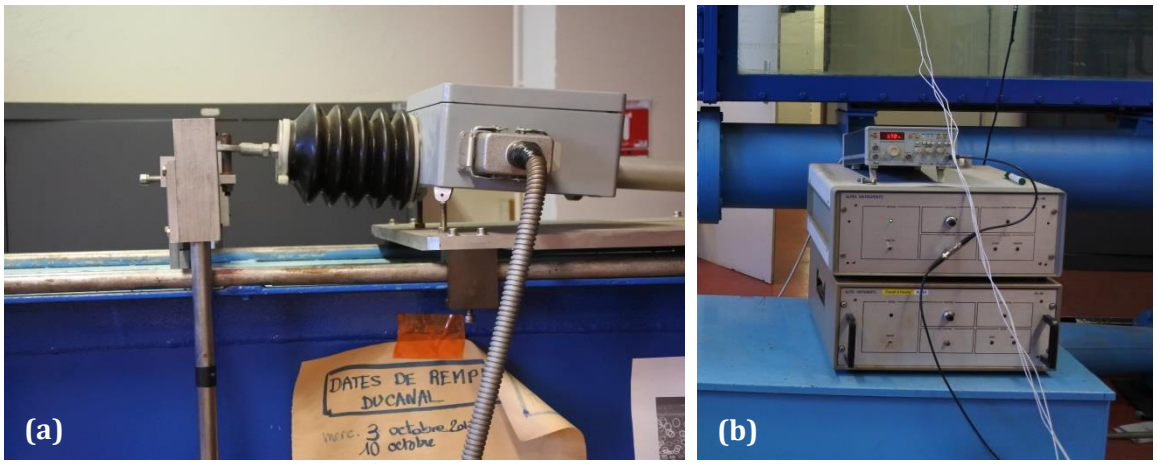

Figure 2 : Pictures of (a) the servomotor controlling flap oscillations and generating the wave trains and (b) its controller

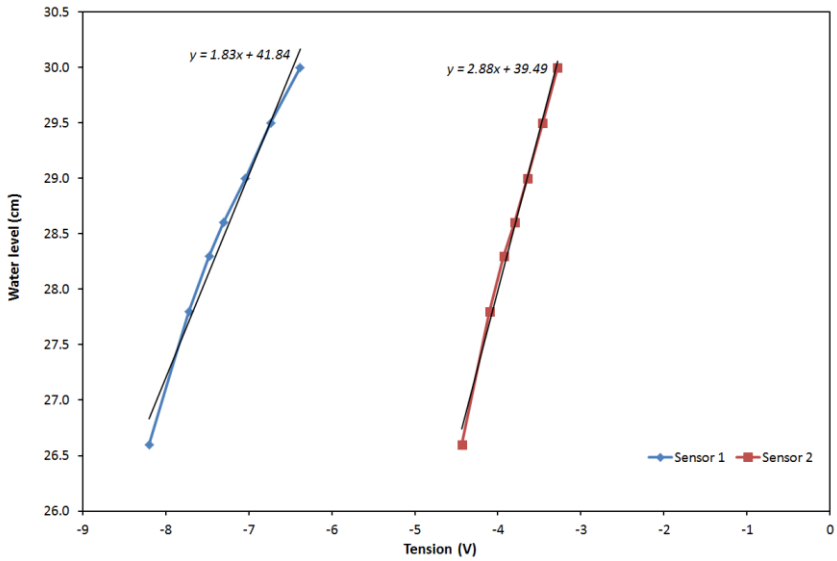

Figure 3: Water level in the wave basin as a function of the voltage measured accross the Wheatstone bridge. Linear fits on the plot indicate the calibration laws that were used in the experiments.

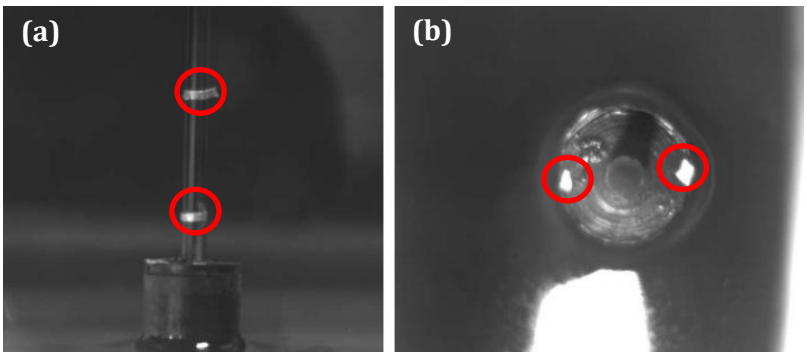

Figure 4 : (a) Side view and (b) top view of the floating structure filmed by two cameras. Light markers on each image are tracked to derive floater motion time series

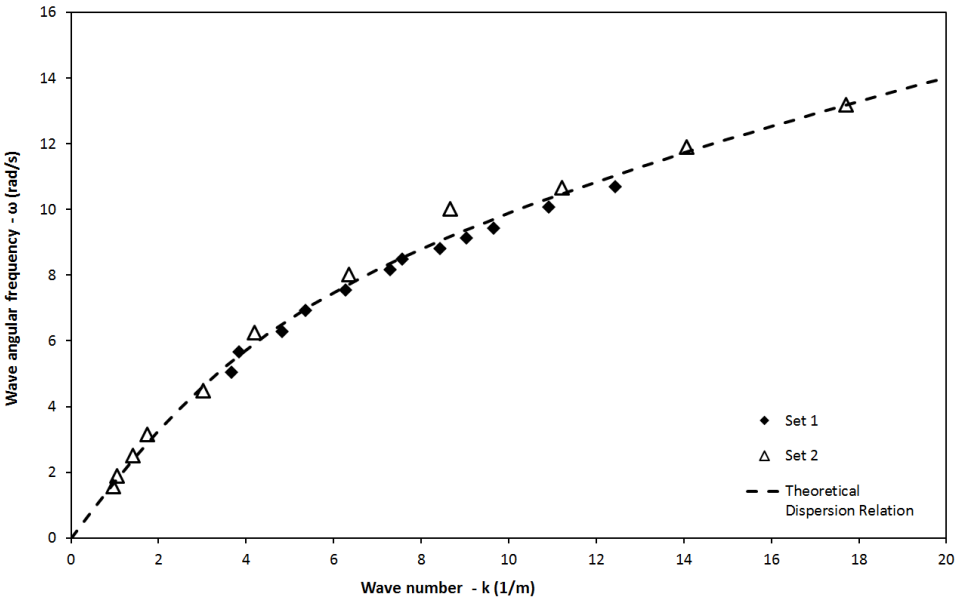

Figure 5: Dispersion relation for the considered wave basin. The theoretical value is shown in the dashed line, while two different sets of experiment are shown using triangles and square symbols

a. Scaling law

When designing a reduced-scale model, there are different dimensionless parameters that ideally have to be kept constant in order to accurately represent the reality of the physical mechanisms that are investigated.

In the present set of experiments, there are three main parameters that can be identified: the Froude number, the Keulegan-Carpenter number, which scales the typical size of the floating structure and the relative displacement of the fluid particles around the structure, and the Stokes number, which is a Reynolds number based on the velocity amplitude of the oscillating fluid particles. Unfortunately, these parameters cannot be kept constant simultaneously when changing scale.

As it was expected that the viscosity played a minor role compared to gravity and inertia effects, even in our small scale experiments, we adjusted geometries in a way so that the Keulegan-Carpenter number and the Froude number are kept constant. It was moreover

already stated that the size of the wave flume imposes quite severe constraints on the size of the model due to wall effects and blockage, and therefore on the choice of the scaling factor. Finally, a Froude scaling, keeping both the Froude number and the Keulegan-Carpenter number constant, was selected with a very small scaling factor of 1/500 imposed by the width of the wave flume. This justifies the question at the start of the present study of the interest of such very-small scale experiments when it comes to gather information on the dynamic behaviour of a real-size structure.

b. Small-scale model

The objective of the experimental campaign is to estimate the interest of the performed tests to investigate the dynamics of realistic floating wind turbine. It was consequently important to consider a realistic design. A typical semi-submersible tri-floater was selected, with a design inspired by DeepCwind floating wind system, [1]. This floater is moored with three catenary mooring lines, one connected to each of the three floating columns at the corners of the platform, with a 120° spacing between adjacent mooring lines.

The small-scale model considered in the experimental campaign is presented in Figure 6. As already mentioned in Section 2, a 1/500th Froude-scaling law was followed to derive the dimensions of the model. As a consequence, the axis-to-axis distance between columns is 10cm, instead of 50m in reality. As an illustration, the main dimensions of the reduced-scaled model are gathered in Table 1. Moreover, the heave natural period of the model was measured thanks to free-decay tests in the wave basin and was equal to 0.63 s. The surge natural period was too large and the free-decay tests were too quickly damped to allow for an experimental derivation of the natural period. However, this was numerically derived to be equal to 20s.

Table 1: Main dimensions of the 1/500 reduced scale model

Total draft of the floater	[m]	0.040
Column height	[m]	0.052
Column diameter	[m]	0.024
Heave plate height	[m]	0.012
Heave plate diameter	[m]	0.050
Distance between column centers	[m]	0.100
Platform mast including ballast	[kg]	0.113
Mast height	[m]	0.155
Number of mooring lines	[-]	3
Mooring lines diameter	[m]	120
Mooring lines mass per unit length in water	[kg/m]	0.001
Angle between adjacent mooring lines	[°]	120
Height to fairleads from keel	[m]	0.010

The very small-scale of the floater also resulted in some fabrication challenges, which induced several necessary deviations of the model's geometrical and mechanical properties from the real-scale floater it was inspired by. This was especially true for the mooring lines, which should for instance have a 0.1mm diameter according to the scaling law, which was not feasible. The main characteristics defining the mooring systems are in Table 1 and its general layout is shown on Figure 7. Based on the intuition that the weight is the main source of resistive force in presence of low-frequency excitation, the decision was made to have the mass per unit length follow the scaling law even if other criteria (like axial stiffness or diameter

scaling) had to be violated. The mass per unit length of the mooring lines was then conserved through the addition of very small weights along the line. Even if the mass is then discretized, the distribution of the masses was dense enough to reproduce the global behaviour of the line quite accurately.

Finally, the narrow wave flume implies severe restrictions on the overall layout of the mooring, consisting of three catenary lines with a 120° angle between each of the lines. Two of these were consequently deviated to fit within the flume. This was performed through the insertion of two very smooth metallic rods allowing to keep artificial friction low, see Figure 7.

3. Numerical Analysis

In this paper, numerical assessment of the floater's rigid-body motions is performed using CALHYPSO, a code dedicated to the modelling of Floating Offshore Wind Turbine dynamics developed by EDF R&D. CALHYPSO is a time-domain solver able to treat both Horizontal-Axis Wind Turbines (HAWT) and Vertical-Axis Wind Turbines (VAWT), using BEMT and DMST for the computation of aerodynamic forces [5] and sea-keeping techniques for floating system hydrodynamics [8]. Turbine elasticity and gyroscopic effects are taken into account using 1D finite elements.

Hydrostatic restoring forces can be derived from a fully linearized stiffness matrix or by direct integration of the submerged volumes. The hydrodynamic wave forces are obtained by combining strip theory for small members with the linear potential-flow approach for the larger parts of the floater. The diffraction-radiation problem is solved by NEMOH [3] an open-source diffraction-radiation code developed by Ecole Centrale de Nantes, which produces a first-order hydrodynamic database used in the time domain following the Cummins method. Quadratic Transfer Functions (QTF) can also be derived by NEMOH, as presented in [4], and subsequently integrated within CALHYPSO. The wave kinematic models available for use with the strip theory are Stokes 1st, 2nd, 3rd and 5th order for regular wave trains, and Stokes 1st and 2nd order for irregular sea states [6]. Higher-order wave models (Stream function, HOS method) can also be interfaced with CALHYPSO.

Depending on the required level of complexity, the mooring lines can be modelled using a linear stiffness matrix, a semi-analytical quasi-static method based on the catenary equation, or via the finite-element method under large displacements and dynamic assumptions. The modelling choice is based on the available inputs and on the outputs expected by the user. To date, the floater is regarded as rigid (6 degrees of freedom) and the equations of motion can be solved using either explicit Euler and RK4 schemes or the implicit Newmark scheme. Coupling with turbine and mooring dynamics is performed at each sub-iteration. EDF R&D is currently working on flexible floater modelling.

CALHYPSO has been validated by EDF R&D within industrial projects (Vertiwind, PGL), as well as through France Energies Marines project VALEF-2, using various turbine types (HAWT, VAWT) and various floater concepts (barge, tri-floater, SPAR, TLP). In the present paper, as basin tests are focused on hydrodynamics only, the turbine is modelled by its weight and inertia and no aerodynamic or operating forces are considered. Inertial hydrodynamics are modelled using a first-order Hydrodynamic Database (HDB) obtained for the wetted surface presented in Figure 8.

It is essential to note that full-scale dimensions are used in the numerical model and its results are subsequently scaled down for comparison with the basin test data to be compared with the results of the experimental campaign.

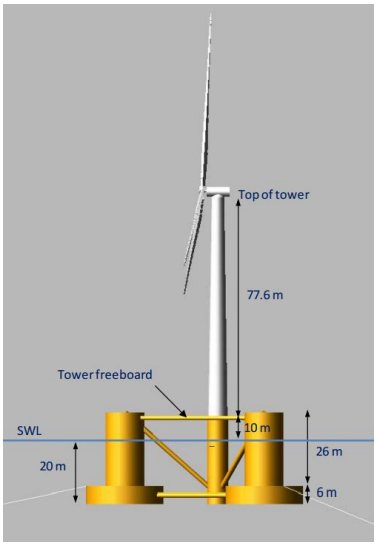

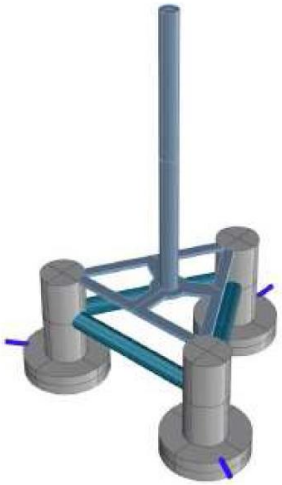

Figure 6: (Left) DeepCwind floater, extracted from [1], from which the small-scale floater (right) was inspired

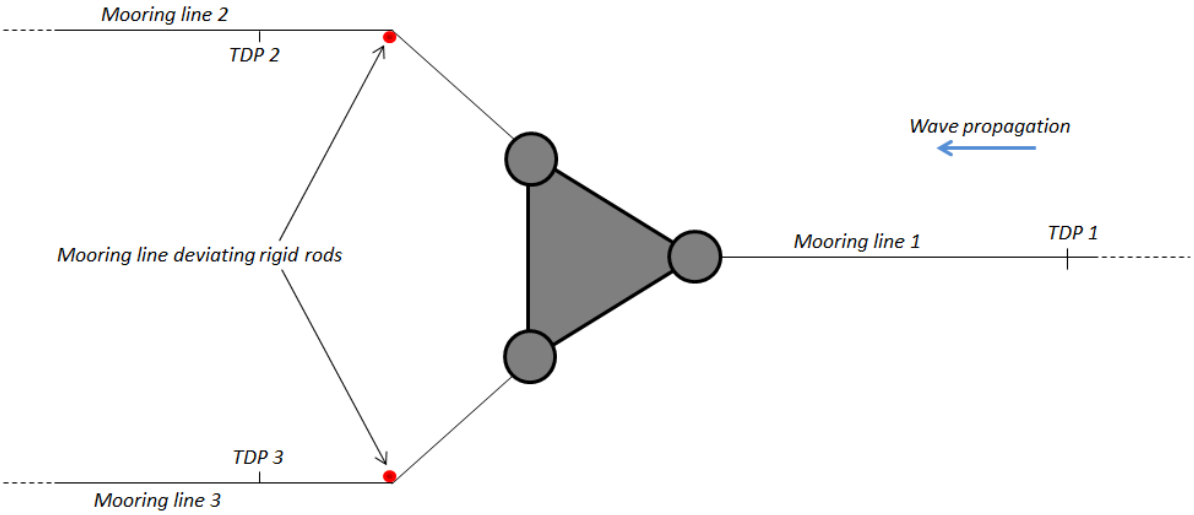

Figure 7: Scheme of the experimental setup with a focus on the mooring system

The HDB contains frequency-dependent Froude-Krylov and diffraction force RAOs, and all radiation damping and added mass coefficients. In addition, viscous forces are superposed using the drag part of the Morison equation, with drag coefficients based on experimental data, and function of Keulegan-Carpenter and Reynolds number pairings calculated at the model scale. For transverse cylinder forces, this requires extrapolation as the pairings do not fall within the reference experimental data set produced by [9]. Additionally, an axial drag coefficient of 5 (calibrated through larger-scale tank tests) is assigned to the lower columns to account for flow separation, based on the assumption that sharp corners lock the separation point thereby limiting the drag coefficient's sensitivity to the Reynolds number. The catenary mooring system is modelled with the quasi-static method, assuming a 120° spaced radial line layout with homogeneous distribution of weight along the lines.

The natural periods in surge and heave obtained with the numerical models are respectively 22.2 s and 0.56 s, corresponding to natural frequencies of respectively 0.05 Hz and 1.79 Hz. It

is interesting to note here that, given the scaling factor of 1/500, this corresponds to a heave natural period at real scale of 12.51 s, similar to waves which could be observed in reality. It would then be of primary importance that this frequency actually belongs to the frequency range covered in the performed analyses, the results of which are described in Section 4.

The numerical model was run for several regular wave cases with durations of up to 8000s, covering the experiments performed at ENSTA-Paristech. A time step of 0.1s is chosen for most of the simulations and the implicit Newmark time integration scheme with $\beta=0.25$ and $\Upsilon=0.5$ has been used. In this case the computational time is really short (<1minute for a load case), as only the 6 degrees of freedom of rigid-body motion are activated. After verification of harmonic behaviour at the steady state, motion RAOs are deduced by applying the max-min approach to the time-domain motion signals at the center of gravity.

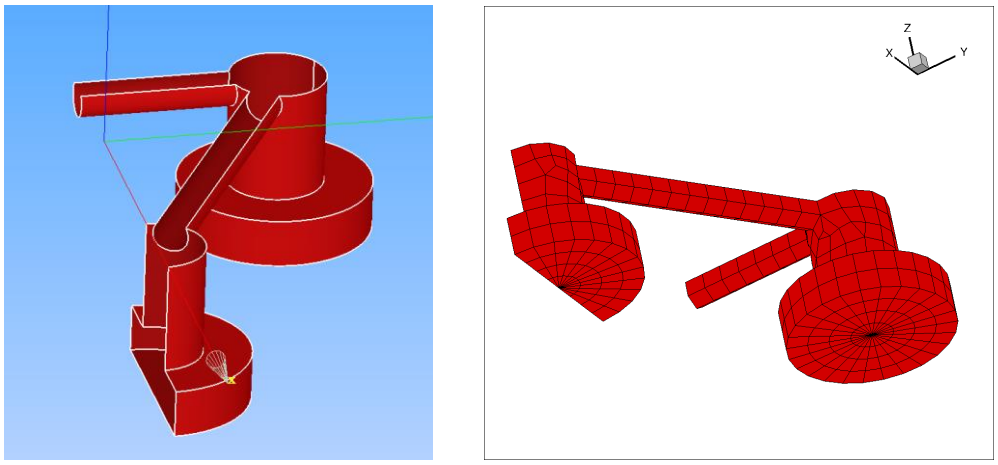

Figure 8: Visualization of the geometry and mesh used for HDB computation

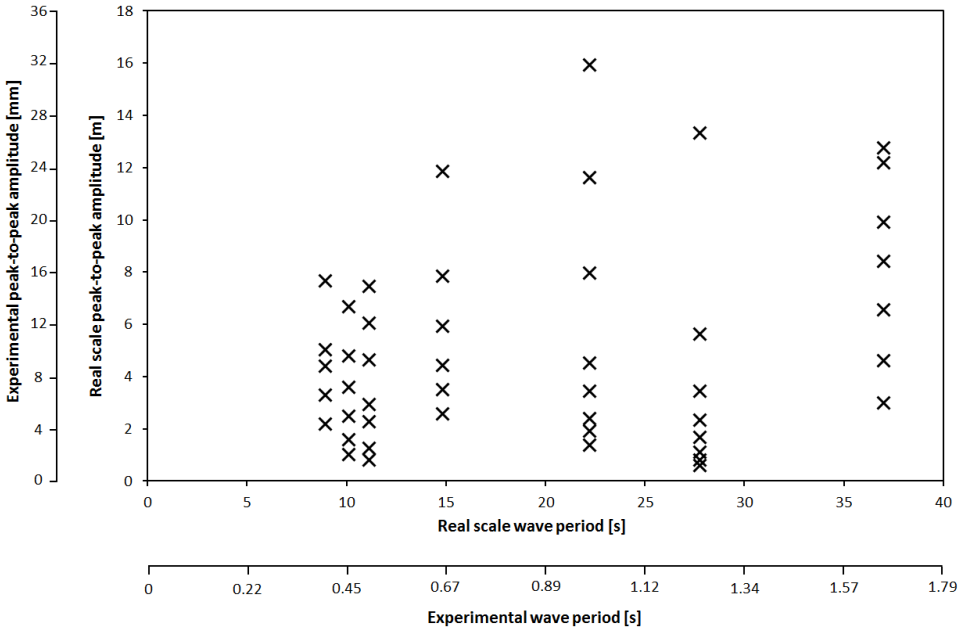

Figure 9: Wave amplitude and period for the tested waves

4. Results

The results from both experimental and numerical analyses are presented in terms of surge, Figure 10, and heave, Figure 11, as functions of the wave frequency, at experimental scale. For each wave, the floater motion was derived according to the protocol described in Section 2. Then the amplitudes for surge and heave degrees of freedom were extracted as

$$A = 2\sqrt{2X_{RMS}} \quad (2)$$

with X_{RMS} the rms average of the motion time series. The amplitudes are normalized by the amplitude of the incoming wave. For each wave frequency, several wave amplitudes were actually tested, as shown on Figure 9. It is also interesting to note here that the covered range of frequencies, going from 0.2 Hz up to 2.5 Hz, corresponds to real-scale wave period between 9s and approximately 37 s, which include classical wave periods observed in the oceans.

a. Surge

The results in terms of surge are shown on Figure 10 and exhibit a very good overall agreement between experimental and numerical plots, with an overall decrease of the normalized response, even if the dependency from the wave amplitude for a fixed frequency is significantly higher for experimental values than for numerical ones.

This could be due to non-linearities in the response, even if this explanation does not appear to be the most probable, considering the high natural period of the floater compared to wave period on which wave height dependency is very pronounced. As numerical simulations were performed at real-scale while experiments considered a very small-scale model, this difference could also be a marker of the impact of some physical mechanisms which impact the dynamics of the floater at small scale but can be neglected at real-scale. This will be discussed in Section 5, even if the uncertainties due to the present experimental protocol are too high to extract some quantitative information from this remark.

a. Heave

The results in terms of heave are shown on Figure 11 and exhibit a rather good agreement between experimental and numerical plots, even if this is not as good as for surge.

Moreover, the overall evolution of the normalized heave response follows a classical trend, with a regular decrease of the response at high frequency and a convergence towards unit at low excitation frequencies. This convergence is not fully achieved for the experimental results, even if a correct tendency is observed. A significant numerical overestimation of response is also observable, which may be related to the linearization of inertial hydrodynamic forces on the horizontal bracings.

However, one can observe a peak in the experimental response at a wave frequency of approximately 0.8Hz, corresponding to a wave period of 28s at real scale, which is not present in the numerical curve. This peak would look like a resonance, but if that was related to the heave natural frequency of the floater, then it would have also appeared on the numerical plot. No clear explanation could be given to explain the presence of this peak in tests and not in simulations, however potential source mechanisms may be sought in diffracted or radiated wave reflections on the flume sides or in anomalies caused by the mooring system. From the

numerical point of view, it is to be underlined that the linear potential-flow model cannot accurately compute the forces acting on the horizontal cylinders which lie on the free surface; non-linearities induced by the non-vertical walls, member emersion, and vertical dynamic pressure balance are not represented. This arrangement could also lead to parametric hydrostatic response of the floater even if this may not be related to the peak in question since the theoretical heave natural frequency associated with the complete immersion/emersion of the horizontal bracings is of 1.2 Hz approximately. For the physical model part, as for the surge degree of freedom, a higher dependency from the wave amplitude of the normalized heave response was also observed for any given frequency. Again, it is hard to derive robust conclusions on that phenomenon from this set of data given the uncertainties in the experiments. More tests would be required to assess whether this deviation is due to uncertainties related to hard-to-control aspects of the experiments at such a small scale or if they really reflect physical couplings playing a significant role at that scale and/or in a confined flume.

5. Conclusions and Discussion

Finally, the dynamics of a typical floater were investigated in terms of surge and heave through both small-scale experiments and numerical simulations considering the equivalent structure at full scale.

The good agreement between the wave basin tests results and the numerical simulations would tend to give credit to such small-scale tests when it comes to giving a first insight of the floater dynamics. Such small-scale tests are indeed very flexible and very easy to implement and could be of high interest as first experimental tests early in the design process in order to help in the convergence towards one (or at least a few) possible designs, to be tested at bigger scale in a much more comprehensive experimental investigation. Also, with the right fabrication precautions, it may be possible to conduct full parametric investigations at a limited cost. However and in spite of this highlighted interest, there are clear limitations to this type of small-scale tests. These are next discussed as potential leads for future work.

i. <u>Model Size and Response Amplitudes</u>
Because of the small size of the model, and of the excitation as the wave amplitudes were of the order of 1cm, the displacements which are to be measured are obviously very small, of the order of 1cm or several millimeters. Sufficiently precise sensors are consequently required to capture such small motions. This was particularly true for rotational degrees of freedom like pitch, roll and yaw, which could not be measured with the camera. A more refined approach would have to be adopted to accurately capture the response of the floater in all 6 degrees of freedom. Additionally, it could have been interesting, for instance, to record the top tension of the mooring lines. Loads were however also way too small to be measurable with classical devices, even with small load cells. A specific sensor will have to be designed to be able to measure this very small force in the context of a 1/500 scale model. This constitutes a clear limitation of small-scale experiments as one must ensure that the studied physical phenomenon can actually be measured at such scale.

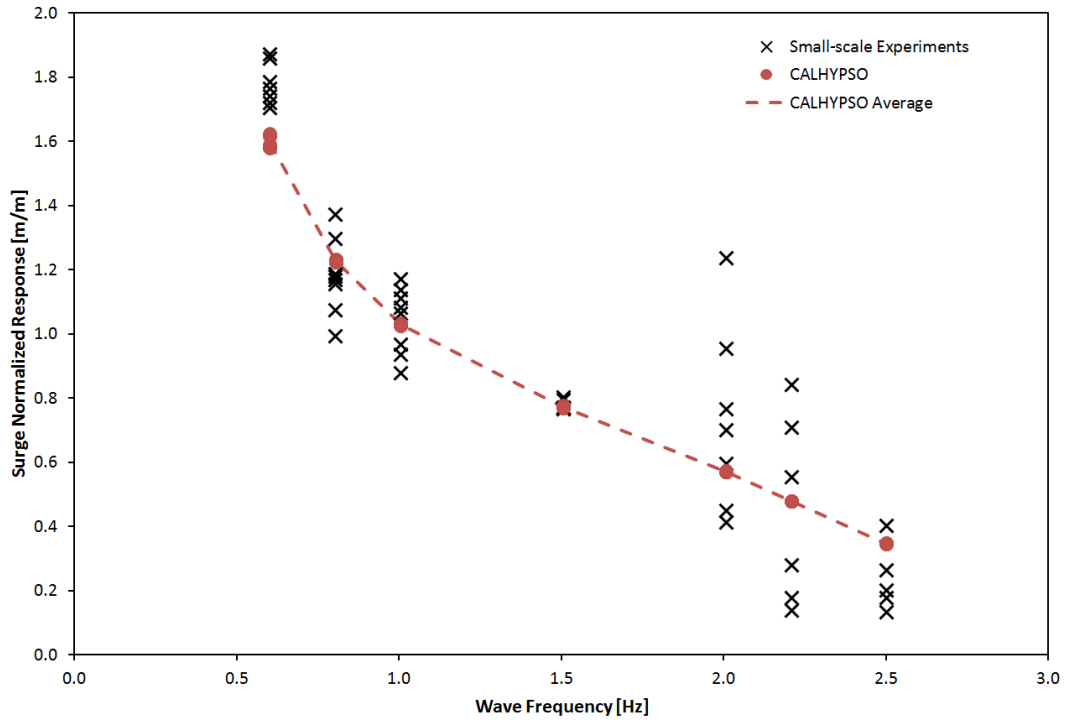

Figure 10: Surge normalized response as a function of the wave frequency, with experimental data (cross), numerical results (dots) and averaged numerical results (dashed line). The theoretical surge natural frequency is 0.045 Hz

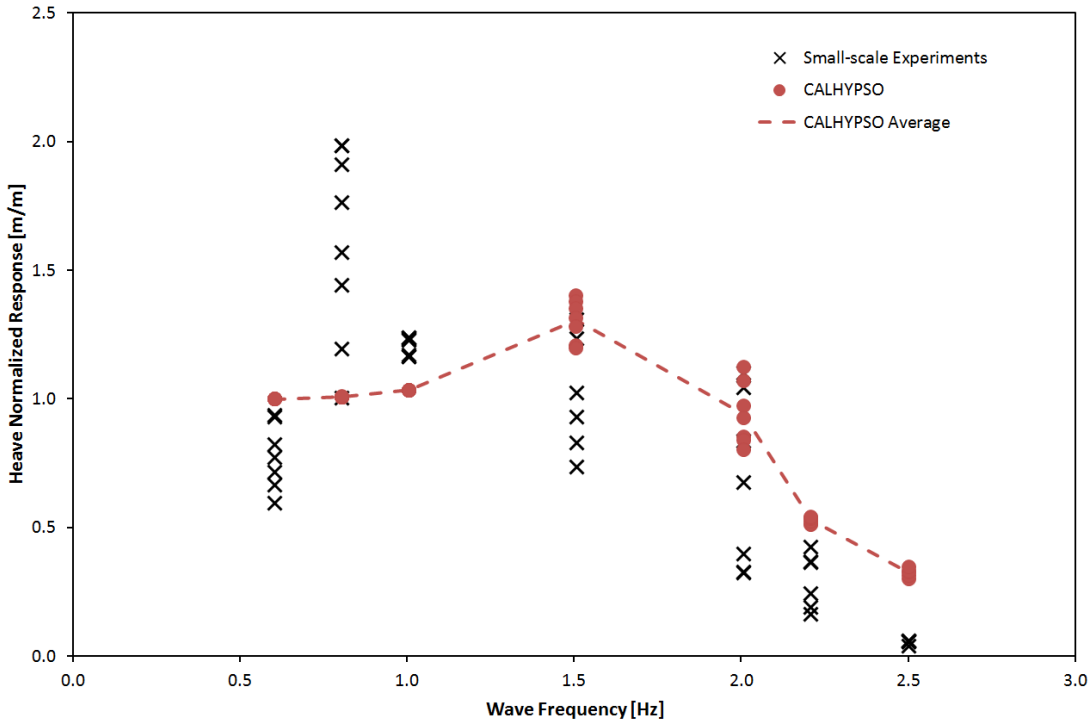

Figure 11: Heave normalized response as a function of the wave frequency, with experimental data (cross), numerical results (dots) and averaged numerical results (dashed line). The theoretical heave natural frequency is 1.787 Hz and the experimentally measured natural frequency is 1.59 Hz.

ii. Blocking

It was previously said that the selection of a scaling factor of 1/500 was mainly driven by the dimensions of the wave basin. Among those dimensions, the width of the wave basin was very narrow and this resulted in some constraints on the experimental device, especially on the mooring system as detailed in Section 2. But this may also impact the results through blocking effects as the model is not so far from the basin walls, through diffracted and radiated wave fields for instance even if only axial uni-directional waves were considered, this may impact the results. The good agreement between the numerical and experimental results would yet tend to mitigate this limitation as an unlimited domain with a full undisturbed mooring system was considered in simulations. Any experimental response feature suspected to derive from wall reflexions may be singled out using finite-domain numerical simulation tools (e.g. a potential-flow numerical wave tank).

iii. Deviations from Scaling Law

As mentioned previously, it was not possible to follow a perfect 1/500th Froude scaling law for the entire tested device, especially in terms of mechanical properties of the structure and mooring lines. This may have an impact on the dynamical response of the floater even if it sounds a reasonable approximation for a conceptual design phase to consider a rigid floater and to focus on the weight of the mooring lines since, from the floater dynamics point of view, this is the main source of restoring force for the tested wave frequencies.

iv. Absence of wind

In this paper, no wind action has been considered. From the experimental point of view it was necessary to address the specific hydrodynamic issue before moving to aerodynamic-hydrodynamic coupling. Clearly, wind-induced loads are expected to produce significant floater motions and may be more significant than hydrodynamic loads in several operating cases. Nonetheless, it appears very difficult to perform scaled experiments of a realistic turbine on a floater, even at larger scales such as 1/20th. Aerodynamic loads are governed by the Reynolds number, which is strongly affected by Froude scaling; this has notably prompted aerodynamic set-up workarounds such as modified blade pitch distribution, thrust-matched adjustment of the wind speed, and the use of low-Reynolds blade geometries. For investigation and simple assessment of aerodynamic-hydrodynamic coupling, one could consider using a porous disc to model the turbine drag force, potentially complemented by rotating masses to simulate the rotor's gyroscopic properties. Another promising way to approach the problem may be the use of a "hardware in the loop" method, which allows the introduction of rotor forces through actuators controlled by aerodynamic simulation software. Here again, very small scale would require computing and imposing the aerodynamic forces on the model with very small latency.

v. Surface Tension

One specific concern of the present experimental study is the potential for appearance of surface tension effects at the very small scale used in the ENSTA-Paris wave flume. It is specified in [7] that the surface tension can play a significant role in experiments with waves when the wavelength is lower than some centimeters. A typical value of 1.7 cm is deduced from the modified dispersion relation. In the present case this would lead to a full-scale wave length of 8.5m (2.5s wave period), and could have an impact on irregular sea state modelling for example. In the present study, only larger wavelengths have been considered. Of course, at this scale it would also be necessary to pay attention to the specific wave-structure interaction issue, with focus on the free surface distortion close to the body. It is difficult to estimate to what extent the surface tension may be held responsible for the presently observed numerical/experimental mismatches, as other sources of uncertainties arise from measurements and, of course, from the assumptions underpinning the numerical model.

vi. Range of investigated parameters and extrapolation

One main limitation of such small-scale tests comes from the inconsistency between Reynolds and Froude scaling. Indeed, as mentioned in Section 2, it is not possible to preserve both Froude number and Reynolds or Stokes number. As a consequence, the dimensionless parameters driving the physical response of the system are not the same for tests at they are in reality. However, it is proven in [7] or [9] that the viscous hydrodynamic loads on a typical structure actually depend on this Stokes number, which would vary with the scaling factor at the power 3/2, which could lead to significant difference in the flow regime then in the dynamic loads on the structure. This constitutes a strong limitation of small-scale experimental campaigns, which has to be kept in mind in their planning.

6. References

[1] J.B. Lacaze & Al. (2014), *Small Scale Tests of Floating Wind Trubines in the Wind and Wave Flume of Luminy,* Proceedings des 14e journées de l'hydrodynamique, Val de Reuil, 18 -20th Nov 2014

[2] A. Robertson & Al. (2014), *Definition of the Semisubmersible Floating System for Phase II of OC4,* NREL Technical Report

[3] Ecole Centrale de Nantes. LHEEA - NEMOH. Online : http ://lheea.ec-nantes.fr/doku.php/emo/nemoh/start. Accessed : June 2014.

[4] M. Philippe & Al. (2015) *Introducing Second Order Low Frequency Loads in the Open-Source Boundary Element Method Code Nemoh,* Proceedings of the 11th European Wave and Tidal Energy Conference 6-11th Sept 2015, Nantes, France

[5] R. Antonutti & Al. (2014), *Aerodynamic Damping Effect On The Motions Of A Vertical-Axis Floating Wind Turbine*, Proceedings des 14e journées de l'hydrodynamique, Val de Reuil, 18 - 20th Nov 2014

[6] G.Z Forristall (2000) *Wave Crest Distributions: Observations and Second-Order Theory*, Journal of Physical Oceanography, Vol 30(8) pp1931-1943

[7] B. Molin (2002), *Hydrodynamique des structures offshore*, Ed.Technip

[8] R. Antonutti & al. (2016), *The Effects Of Wind-Induced Inclination On The Dynamics Of Semi-Submersible Floating Wind Turbines In The Time Domain*, Renewable Energy, vol. 88, pp. 83–94

[9] T. Sarpkaya and M. Isaacson (1981), *Mechanics of Wave Forces on Offshore Structures,* New York, USA: Van Nostrand Reinhold Co.